

# miR-128-3p enhances the protective effect of dexmedetomidine on acute lung injury in septic mice by targeted inhibition of MAPK14

Li Ding (✉ [dingli23hh@163.com](mailto:dingli23hh@163.com))

The People's Hospital of Yinzhou <https://orcid.org/0000-0002-2988-2153>

Xiang Gao

The People's Hospital of Yinzhou

Shenghui Yu

The People's Hospital of Yinzhou

Liufang Sheng

The People's Hospital of Yinzhou

---

## Research article

**Keywords:** miR-128-3p, MAPK14, dexmedetomidine, sepsis, acute lung injury

**Posted Date:** March 3rd, 2020

**DOI:** <https://doi.org/10.21203/rs.3.rs-15885/v1>

**License:**   This work is licensed under a Creative Commons Attribution 4.0 International License.

[Read Full License](#)

---

**Version of Record:** A version of this preprint was published at Journal of Bioenergetics and Biomembranes on June 27th, 2020. See the published version at <https://doi.org/10.1007/s10863-020-09842-8>.

# Abstract

**Background:** To investigate the role of miR-128-3p and MAPK14 in the dexmedetomidine treatment of acute lung injury in septic mice.

**Methods:** SPF C57BL/6 mice were divided into 8 groups. The pathological changes and wet/dry weight ratio (W/D), PaO<sub>2</sub>, PaCO<sub>2</sub>, MDA, SOD and MPO levels in lung tissue and the serum levels of inflammation factors were observed. Dual luciferase reporter assay was used to detect the targeting relationship of miR-128-3p and MAPK14, and qPCR and WB were used to detect the expression of miR-128-3p and MAPK14.

**Results:** Compared with the Normal group, other groups had lower MDA, MPO, inflammatory factors levels and the expression level of MAPK14, while the content of SOD and the expression level of miR-128-3p was significantly decreased (all  $p < 0.05$ ). Compared with the Model group, the contents of MDA, MPO, inflammatory factors in the DEX group and miR-128-3p mimic group were significantly decreased, and the content SOD was significantly increased, however, opposite results were occurred in oe-MAPK14 group (all  $p < 0.05$ ). Compared with the DEX group, all the indicators in miR-128-3p mimic+DEX group showed significant improvement (all  $p < 0.05$ ). Compared with the miR-128-3p mimic group, all the indicators were deteriorated in the miR-128-3p mimic+oe-MAPK14 group (all  $p < 0.05$ ). The combination of DEX and oe-MAPK14 blocked the protective effect of dexmedetomidine on acute lung injury in septic mice.

**Conclusion:** miR-128-3p can further enhance the protective effect of dexmedetomidine on acute lung injury in septic mice by targeting and inhibiting MAPK14 expression.

## Background

Sepsis is the most common systemic clinical complication of severe trauma, burns and major surgery, which can deteriorate into multiple organ dysfunction syndrome, becoming the leading cause of death in these patients [1]. Traditionally, sepsis is considered to be an organ failure syndrome caused by immune disorders in the case of severe infection [2]. Excessive inflammatory response induced by sepsis can lead to multiple organ damage and failure. Acute lung injury (ALI) is a common complication of sepsis as lung is particularly sensitive to sepsis damage [3]. ALI is characterized by progressive hypoxemia, enhanced vascular permeability, edema, neutrophil infiltration and lung accumulation, which greatly increases patient morbidity and mortality [4]. Therefore, the researches on the new targets for the treatments of sepsis are hotspot [5].

Dexmedetomidine (DEX), a  $\alpha_2$ -adrenergic receptor agonist, has an imidazole structure and sedative, analgesic and hemodynamic stabilization effects [6]. A good anti-inflammatory effect of DEX has been discovered on important organs in mice with spinal cord injury, myocardial ischemia-reperfusion and sepsis, etc. [7]. Moreover, DEX can improve ALI, reduce pathomorphological changes, inhibit oxidative

stress damage, inflammatory response and apoptosis in lung epithelial cells by inhibiting TLR-4/NF- $\kappa$ B pathway [8].

MicroRNAs (miRNAs) are endogenous small non-coding RNAs with a length of 21–23 nucleotides. miRNAs inhibit translation or induce the degradation of targeted mRNA by binding to the 3' untranslated region (UTR) [9]. Increasing number of evidences have proved that miRNAs associated with certain inflammatory lung diseases. For example, up-regulation of miR-125b significantly reduced lipopolysaccharide (LPS)-induced lung inflammation in mice [10]. miR-212-3p inhibits LPS-induced inflammatory responses by targeting high mobility group box – 1 in mouse macrophages [11]. miR-128-3p plays an important role in Dox-induced liver injury by targeting Sirt1 [12]. However, whether miR-128-3p participates in the anti-inflammatory activity of dexmedetomidine in ALI remains unclear.

ALI is often mediated by a variety of intracellular signaling pathways, such as PI3K/Akt, c-Jun N-terminal protein kinase, mitogen-activated protein kinase, and p38 activation, which play a role in inflammatory responses, cell death, and alveolar epithelial cell damage in ALI [13, 14]. P38 mitogen-activated protein kinase (p38MAPK) is an important signal regulating cell proliferation and apoptosis. Its phosphorylated form can activate a variety of physiological processes, and MAPK14 is a member of the MAPK family [15]. In this study, we found a targeting relationship between miR-128-3p and MAPK14 via bioinformatics prediction. We hypothesized that miR-128-3p may down-regulate the expression of MAPK14, thereby inhibiting p38 signaling pathway to alleviate ALI in septic mice.

Therefore, we established a sepsis model and treated them with miR-128-3p overexpression vectors, dexmedetomidine, MAPK14 overexpression vectors, or their combinations to explore whether miR-128-3p will affect the p38MAKE pathway and play a role in acute lung injury in septic mice.

## Methods

### Animals and model establishment

A total of 120 healthy SPF C57BL/6 mice (purchased from Zhejiang Experimental Animal Center), clean grade, body weight  $35 \pm 5$  g, were used for experiment in this study. Mice were divided into 8 groups: Normal group (healthy mice without treatment), Model group (model mice), DEX group (model mice treated with dexmedetomidine), miR-128-3p mimic group (model mice treated with miR-128-3p overexpression vectors), oe-MAPK14 group (model mice treated with MAPK14 overexpression vectors), miR-128-3p mimic + oe-MAPK14 group (model mice treated with miR-128-3p and MAPK14 overexpression vectors), miR-128-3p mimic + DEX group (model mice treated with miR-128-3p overexpression vector and dexmedetomidine), DEX + oe-MAPK14 group (model group mice treated with MAPK14 overexpression vector and dexmedetomidine), with ten mice in each group.

The sepsis model was established by cecal ligation and puncture. Briefly, the mice were fixed in table and anesthetized with 3% pentobarbital sodium (50 m/kg). After eyeball blood collection, the mice died of excessive blood loss, and lung tissue samples were retained. A 1 cm long surgical incision was made in

the central part of the anterior abdominal cavity of the mice to separate out the cecum end, then the root of the cecum was ligated and punctured with a 4-gauge needle, and the contents in cecum were extruded out. Finally, the cecum and incision were sutured. Pre-warmed saline was injected postoperatively. Except for no ligation and puncture, the other steps in the Normal group were the same as those in the model group. Thirty-two animals died, so the success rate of model establishment was 70.90%, of which 70 were taken for the following experiments.

After the operation, mice intraperitoneally injected with DEX (12.5 µg/kg, GLP BIO, America) and miR-128-3p mimic, MAPK14 overexpression vectors (The NC, miR-128-3p and MAPK14 overexpression adenoviral vectors were constructed by GenePharma, Suzhou). After modeling and treatment, lung tissue and venous blood were taken from 5 mice in each group, and some lung tissues were fixed in 10% neutral formalin solution for 24 hours, and was dehydrated by gradient alcohol, embedded in paraffin and sliced. This study was performed in The People's Hospital of Yinzhou, and experimental studies in accordance with the Basel declaration have been approved by the ethics committee of The People's Hospital of Yinzhou (No. D20181103).

## Dual luciferase reporter system assay

The targeting relationship and binding site of miR-128-3p and MAPK14 was analyzed via the biological prediction website ([www.targetscan.org](http://www.targetscan.org)), when was next verified by the dual luciferase reporter system assay. The MAPK14 (PGL3-MAPK14wt) and mutants that bind to the miR-128-3p (PGL3-MAPK14mut) dual luciferase reporter vectors were separately constructed. The Rellina plasmids and the two reporter plasmids were co-transfected into HEK293T cells with the miR-128-3p plasmid and the NC plasmid, respectively. After 24 h of cell transfection, dual luciferase assays were performed according to the instruction of the dual luciferase reporter kit (Promega). Relative luciferase activity = firefly luciferase / Renilla luciferase [8].

## qRT-PCR

Trizol (Thermo Fisher Scientific, New York, USA) was used to extract total RNAs from lung tissue. The cDNA was synthesized by reverse transcription using TaqMan MicroRNA Assays Reverse Transcription Primer (Thermo scientific, USA). SYBR® Premix ExTaq™ II Kit (Xingzhi Biotechnology Co., Ltd., China) was used for quantitative PCR detection. The following components were added in sequence: 25 µL of SYBR Premix ExTaq™ II (2×), 2 µL of PCR upstream and downstream primers, ROXReferenceDye (50×) 1 µL, 4 µL DNA template, and 16 µL of ddH<sub>2</sub>O. Fluorescence quantitative PCR was performed in ABI PRISM® 7300 (model Prism® 7300, Shanghai Kunke Instrument Equipment Co., Ltd., China). The reaction conditions were: pre-denaturation at 95 °C for 10 min, denaturation at 95 °C for 15 s, annealing at 60 °C for 30 s, 32 cycles, extending at 72 °C for 1 min. miR-128-3p with U6 as internal reference, and MAPK14 used GAPDH as internal reference. The relative expression amount of each gene of interest was calculated by  $2^{-\Delta\Delta C_t}$ . Primer sequences are shown in Table 1.

Table 1  
Primer sequences

Gene	Sequence
miR-128-3p	F: 5'-GGTC ACAGTGAACCGGTC-3'
	R: 5'-GTGCAGGGTCC GAGGT-3'
MAPK14	F: 5'-CTGACCGACGACCACGTTC-3'
	R: 5'-CTTCGTTACAGCTAGGTTGC-3'
U6	F: 5'-CTCGCTTCGGCAGCACA-3'
	R: 5'-AACGCTTCACGAATTTGCGT-3'
GAPDH	F: 5'-TTCAACGGCACAGTCAAGG-3'
	R: 5'-CACCAGTGGATGCAGGGAT-3'

## Western blot

Total protein in lung tissue was extracted using RIPA lysate containing PMSF (R0010, solarbio). The protein concentration was determined by BCA kit (thermo, USA). The protein sample was mixed with the loading buffer, boiled for 10 min. Then 50 µg of protein sample was electrophoresed at 70 V for 3 h and transferred onto a PVDF membrane (ISEQ00010, Millipore, Billerica, MA, USA) with constant flow 150 mA. The membrane was then blocked by 5% skim milk at 4 °C for 2 h, washed with TBST, and incubated with anti-rabbit anti-mouse MAPK14 (ab31828, 1:500, Abcam, UK), GAPDH (ab22555, 1:2,000, Abcam, UK) overnight at 4 °C. After washing with TBST thrice, the membrane was incubated with HRP-labeled goat anti-rabbit IgG antibody (Beijing Zhongshan Biotechnology Co., Ltd., diluted 1:5,000) for 2 h and wash TBST thrice. ECL fluorescence detection kit (Cat. No. BB-3501, Ameshame, UK) was used for color development and the membrane was photographed by Bio-Rad image analysis system (BIO-RAD, USA) and the results were analyzed by Image J software. The relative protein content = the gray value of the corresponding protein band / the gray value of the GAPDH protein band.

## Blood gas analysis and lung tissue wet / dry weight ratio (W/D)

The carotid artery blood was taken for blood gas analysis to observe arterial oxygen partial pressure (PaO<sub>2</sub>) and carbon dioxide partial pressure (PaCO<sub>2</sub>). The wet / dry weight ratio (W/D) was calculated to reflect the degree of edema of the lung. The left lung of the mouse was removed by thoracotomy, and the wet weight was weighed after clearing the lung surface by filter paper. After drying in an incubator at 80 °C for 48 h, the sample in constant weight was weighted as the dry weight. Lung tissue wet / dry weight (W/D) = (lung wet weight / lung dry weight) \* 100%.

## HE staining

After modeling and treatment, some lung tissues were fixed in 10% neutral formalin solution for 24 hours, and was dehydrated by gradient alcohol, embedded in paraffin and sliced. Then slice was treated with xylene transparent, hydrated by gradient alcohol and washed with distilled water for 1 min. Subsequently, the slice was stained with hematoxylin for 3 min, flushed with tap water, immersed in alcohol containing 0.5% hydrochloric acid for 10 s, stained with eosin dye solution for 5 min. Finally, the slice was conventionally dehydrated, transparentized and sealed with neutral gum. Each slice was observed under an optical microscope (XP-330, Shanghai Bingyu Optical Instrument Co., Ltd., Shanghai, China).

## **Activity detection of myeloperoxidase (MPO), mitochondrial superoxide dismutase (SOD) and malondialdehyde (MDA)**

The lung tissue in size of 125 mm<sup>3</sup> was homogenized with 1 mL of PBS, centrifuged at 4 °C, 12,000 xg for 10 min, and the supernatant was taken. The myeloperoxidase (MPO), which reflects the degree of neutrophil accumulation in lung tissue, was detected in strict accordance with the kit instructions (K744-100, Biovision, US). MDA and SOD in lung tissue were detected by MDA (A003-1-2) and SOD (A001-3-2) assay kits purchased from Nanjing Jiancheng Reagent Co., Ltd., respectively.

## **Enzyme-linked immunosorbent assay (ELISA)**

Blood taken from mouse eyeballs were stand at room temperature for a while and at 4 °C overnight, centrifuged at 3,500 xg/min to collect serum and the samples were preserved at -80 °C. The level of inflammatory factors was measured by according the ELISA kit instructions (kit numbers: 69-21138, 69-22800, 69-25328, 69-40133; Wuhan Merck, China).

## **Statistical analysis**

All data were processed by SPSS21.0 statistical software. The measurement data were expressed as mean ± standard deviation. One-Way ANOVA and Tukey post- Hoc test was used for comparison between groups.  $p < 0.05$  indicates that the difference is statistically significant.

## **Results**

### **Pathological changes of lung tissue in each group of mice**

HE staining was used to detect the pathological changes of lung tissue in mice (Fig. 1). Lung tissue of Normal group was in regular structure without obvious pathological damage. In Model group, oe-MAPK14 group, miR-128-3p mimic + oeMAPK14 group, there were different degrees of inflammatory cell infiltration in the alveoli and interstitial; there was effusion in the cavity and thickened alveolar septum, meanwhile, some alveoli were collapsed, atelectasis, and formed transparent membrane and alveolar structure was damaged. However, the lung tissue damage of the mice in the DEX group and the miR-128-3p mimic + DEX group was significantly improved compared with the above three groups. The degree of lung tissue damage in the DEX + oe-MAPK14 group was similar to that in the Model group.

## Blood gas analysis and W/D of each group of mice

The W/D of the lung tissue,  $\text{PaO}_2$  and  $\text{PaCO}_2$  of each group are shown in Fig. 2. Compared with the Normal group, W/D,  $\text{PaCO}_2$  was significantly higher and  $\text{PaO}_2$  was significantly lower in the other groups (all  $p < 0.05$ ). Compared with the Model group, W/D,  $\text{PaCO}_2$ , and  $\text{PaO}_2$  showed no significant differences in miR-128-3p mimic + oe-MAPK14 group, in addition, W/D and  $\text{PaCO}_2$  were significantly decreased and  $\text{PaO}_2$  was significantly increased in DEX group, miR-128-3p mimic group, miR-128-3p mimic + DEX group, while opposite results occurred in oe-MAPK14 group ( $p < 0.05$ ). Compared with the miR-128-3p mimic group, the W/D and  $\text{PaCO}_2$  decreased and  $\text{PaO}_2$  increased in the miR-128-3p mimic + DEX group, but the miR-128-3p mimic + oe-MAPK14 group has opposite results (both  $p < 0.05$ ). Compared with the DEX group, the W/D and  $\text{PaCO}_2$  increased and  $\text{PaO}_2$  decreased in the DEX + oe-MAPK14 group (all  $p < 0.05$ ).

## Serum levels of inflammatory factors in mice

The serum levels of inflammatory factors in each group were detected by ELISA (Fig. 3). Compared with the Normal group, the serum levels of inflammatory factors (interleukin (IL)-8, IL-17, IL-6 and tumor necrosis factor (TNF)- $\alpha$ ) were significantly higher in the other groups ( $p < 0.05$ ). Compared with the Model group, there was no significant difference in serum inflammatory factors in miR-128-3p mimic + oe-MAPK14 group, which were significantly lower in DEX group, miR-128-3p mimic group, miR-128-3p mimic + DEX group ( $p < 0.05$ ), but the oe-MAPK14 group had opposite results ( $p < 0.05$ ). Compared with miR-128-3p mimic group, the serum levels of inflammatory factors were significantly less in miR-128-3p mimic + DEX group, but opposite results occurred in miR-128-3p mimic + oe-MAPK14 group ( $p < 0.05$ ). Compared with the DEX group, the serum levels of IL-1 $\beta$ , TNF- $\alpha$  and IL-6 in the DEX + oe-MAPK14 group were significantly increased (all  $p < 0.05$ ).

### MPO, SOD and MDA contents in lung tissue of mice in each group

The results of MPO, SOD and MDA in lung tissue of each group showed in Fig. 4. Compared with the Normal group, the SOD content was significantly lower in the other groups, while the MPO and MDA contents were significantly higher ( $p < 0.05$ ). Compared with the Model group, the content of MPO, SOD and MDA in miR-128-3p mimic + oe-MAPK14 group was not statistically different ( $p > 0.05$ ). SOD content increased and MPO and MDA contents decreased in miR-128-3p mimic group and DEX group when compared with the Model group ( $p < 0.05$ ). The oe-MAPK14 group had opposite results when compared with the Model group ( $p < 0.05$ ). These indicators were in similar trend in miR-128-3p mimic + DEX group but in opposite trend in miR-128-3p mimic + oe-MAPK14 group when compared with miR-128-3p mimic group (all  $p < 0.05$ ). Compared with the DEX group, the serum levels of IL-1 $\beta$ , TNF- $\alpha$  and IL-6 in the DEX + oe-MAPK14 group were significantly increased (all  $p < 0.05$ ).

miR-128-3p targets and negatively regulates the gene expression of MAPK14 and expression of miR-128-3p and MAPK14

The biological prediction website (<http://www.microrna.org/microrna/home.do>) predicted that miR-128-3p and MAPK14 have specific binding sites (Fig. 5a). The dual luciferase report system assay showed (Fig. 5b) that the luciferase activity of the Wt-MAPK14 and miR-128-3p mimic transfected group was significantly lower than that in the Wt-MAPK14 and NC mimic group ( $p < 0.05$ ). However, the luciferase activity of the group transfected with Mut-MAPK14 and miR-128-3p mimic or Mut-MAPK14 and NC mimic group showed no significant difference ( $p > 0.05$ ). Therefore, miR-128-3p could target and negatively regulate MAPK14 gene expression.

To investigate how miR-128-3p protects mouse acute lung injury through p38 signaling pathway, we detected the gene expression of miR-128-3p and MAPK14 by qRT-PCR and Western blot (Fig. 5c-e). Compared with the Normal group, miR-128-3p down-regulated and MAPK14 upregulated in the other groups (all  $p < 0.05$ ). Compared with the Model group, the expression of MAPK14 showed no significant difference in miR-128-3p mimic + oe-MAPK14 group ( $p > 0.05$ ); however, the expression levels of MAPK14 and p-MAPK14 were significantly decreased in miR-128-3p mimic group and DEX group, which increased in oe-MAPK14 group ( $p < 0.05$ ). Compared with miR-128-3p mimic group, the expression levels of MAPK14 and p-MAPK14 significantly decreased in miR-128-3p mimic + DEX group, but increased in miR-128-3p mimic + oe-MAPK14 group ( $p < 0.05$ ); MAPK14 expression level was significantly elevated in the oe-MAPK14 group and the miR-128-3p mimic + oe-MAPK14 group (all  $p < 0.05$ ). miR-128-3p expression level was significantly increased in the miR-128-3p mimic group, the miR-128-3p mimic + DEX group, and the miR-128-3p mimic + oe-MAPK14 group (all  $p < 0.05$ ). Compared with the DEX group, the expression levels of MAPK14 and p-MAPK14 in the DEX + oe-MAPK14 group were significantly increased ( $p < 0.05$ ).

## Discussion

As an invasive disease with a high mortality, sepsis is common in the intensive care unit [16]. Studies have proved that cytokine bursts caused by uncontrolled inflammatory responses could induce severe damage in tissue and organ, even causing death [17]. Acute organ dysfunction is a common respiratory and cardiovascular complication of sepsis [18]. The lung is the easiest infection target in sepsis, which also plays a critical role in the secretion and release of inflammatory mediators [19]. Acute lung injury (ALI) is common complications in clinic, which caused by excessive inflammatory response in the lungs [20]. ALI is characterized by respiratory distress, accompanying with diffuse endothelial and epithelial damage, inflammatory cell infiltration as well as pro-inflammatory cytokines release [21]. Although many attempts have been made to determine new treatment strategies and treatment options for ALI, there are no effective treatments available for clinical use [22]. Therefore, there is an urgent need to develop new ALI treatment strategies and explore possible mechanisms for improving the survival rate of ALI patients.

Dexmedetomidine is a  $\alpha_2$ -adrenergic drug used in clinic, which can be used as an anti-oxidative drug before anesthesia, reducing the concentration of cytokines in kidney tissue and can also reduce lung damage caused by lipopolysaccharide, ischemia-reperfusion and ventilation in animal models [23–25]. Dexmedetomidine has also been shown to reduce oxidative stress and apoptotic lesions in lung tissue [26]. In addition, it can reduce lung tissue fibrosis in rats after acute lung injury [27]. The expression of

miR-128-3p is frequently observed in a variety of human diseases, including myocardial failure, diabetes, etc. [28, 29]. It has been reported that the p38 MAPK signaling pathway is involved in the ALI inflammatory response and mediates the production of many cytokines, including IL-1 $\beta$ , TNF- $\alpha$  and IL-6 [30, 31]. Many anti-inflammatory drugs act by targeting p38 MAPK [32].

In our experiment, we evaluated the protective effect of dexmedetomidine on sepsis-induced lung injury and we found that after the injection of Dex, the expression of MAPK14 was down-regulated, and inflammatory response and oxidative stress damage were alleviated. The protective effect of Dex on ALI was more obvious after overexpression of miR-128-3p. To further explore the molecular regulation mechanism, we confirmed the target relationship between miR-128-3p and MAPK14 and we also found that both miR-128-3p overexpression and Dex can inhibit inflammatory factor release and oxidative stress damage, while overexpression of MAPK14 can reverse the protective effect dexmedetomidine. Therefore, we conclude that overexpression of miR-128-3p in septic mice can target and inhibit P38 signaling pathway and improve the protective effect of dexmedetomidine on acute lung injury in septic mice.

## Conclusions

This study demonstrates that miR-128-3p mediates the P38 signaling pathway by targeting the MAPK14 gene, thereby inhibiting inflammatory factor release and oxidative stress damage. The pathogenesis of acute lung injury was further elucidated in this study, which laid a theoretical foundation for the treatment of acute lung injury induced by sepsis in clinic. To further confirm the above results, we need further research to explore how dexmedetomidine specifically acts on the P38 signaling pathway.

## Abbreviations

W/D, wet/dry weight ratio; PaO<sub>2</sub>, arterial oxygen partial pressure; PaCO<sub>2</sub>, carbon dioxide partial pressure; ALI, acute lung injury; DEX, dexmedetomidine; miRNAs, microRNAs; UTR, untranslated region; LPS, lipopolysaccharide; p38MAPK, p38 mitogen-activated protein kinase; MPO, myeloperoxidase; SOD, superoxide dismutase; MDA, malondialdehyde; ELISA, enzyme-linked immunosorbent assay; ICU, intensive care unit; IL, interleukin; TNF, tumor necrosis factor.

## Declarations

### Ethics approval

This study was performed in The People's Hospital of Yinzhou, and was approved by the Ethics Committee of The People's Hospital of Yinzhou (No. D20181103).

## Consent for publication

Not applicable.

## Availability of data and material

The datasets used and/or analysed during the current study are available from the corresponding author on reasonable request.

## Competing interests

The authors declare that they have no competing interests.

## Funding

Not applicable.

## Authors' contributions

LD and LFS were responsible for data collection and data process. XG and SHY contributed to statistical analysis and data analysis. LD was responsible for manuscript concept, guidance and editing. All authors read and approved the final manuscript.

## Acknowledgements

Not applicable.

## References

1. Zhuo Y, Li D, Cui L, Li C, Zhang S, Zhang Q, et al. Treatment with 3,4-dihydroxyphenylethyl alcohol glycoside ameliorates sepsis-induced ALI in mice by reducing inflammation and regulating M1 polarization. *Biomed Pharmacother*. 2019;116:109012.
2. Iwaki T, Bennion BG, Stenson EK, Lynn JC, Otinga C, Djukovic D, et al. PPARalpha contributes to protection against metabolic and inflammatory derangements associated with acute kidney injury in experimental sepsis. *Physiological reports*. 2019;7:e14078.

3. Peng QY, Zou Y, Zhang LN, Ai ML, Liu W, Ai YH. Blocking Cyclic Adenosine Diphosphate Ribose-mediated Calcium Overload Attenuates Sepsis-induced Acute Lung Injury in Rats. *Chinese Medical Journal*. 2016;129:1725-30.
4. Mehaffey JH, Charles EJ, Sharma AK, Salmon M, Money D, Schubert S, et al. Ex Vivo Lung Perfusion Rehabilitates Sepsis-Induced Lung Injury. *Ann Thorac Surg*. 2017;103:1723-9.
5. Acosta-Herrera M, Lorenzo-Diaz F, Pino-Yanes M, Corrales A, Valladares F, Klassert TE, et al. Lung Transcriptomics during Protective Ventilatory Support in Sepsis-Induced Acute Lung Injury. *PLoS One*. 2015;10:e0132296.
6. Zhang Q, Wu D, Yang Y, Liu T, Liu H. Dexmedetomidine Alleviates Hyperoxia-Induced Acute Lung Injury via Inhibiting NLRP3 Inflammasome Activation. *Cell Physiol Biochem*. 2017;42:1907-19.
7. Zhang H, Sha J, Feng X, Hu X, Chen Y, Li B, et al. Dexmedetomidine ameliorates LPS induced acute lung injury via GSK-3 $\beta$ /STAT3-NF- $\kappa$ B signaling pathway in rats. *Int Immunopharmacol*. 2019;74:105717.
8. Meng L, Li L, Lu S, Li K, Su Z, Wang Y, et al. The protective effect of dexmedetomidine on LPS-induced acute lung injury through the HMGB1-mediated TLR4/NF- $\kappa$ B and PI3K/Akt/mTOR pathways. *Mol Immunol*. 2018;94:7-17.
9. Jin Y, Yang C, Sui X, Cai Q, Guo L, Liu Z. Endothelial progenitor cell transplantation attenuates lipopolysaccharide-induced acute lung injury via regulating miR-10a/b-5p. *Lipids Health Dis*. 2019;18:136.
10. Guo Z, Gu Y, Wang C, Zhang J, Shan S, Gu X, et al. Enforced expression of miR-125b attenuates LPS-induced acute lung injury. *Immunol Lett*. 2014;162:18-26.
11. Chen W, Ma X, Zhang P, Li Q, Liang X, Liu J. MiR-212-3p inhibits LPS-induced inflammatory response through targeting HMGB1 in murine macrophages. *Exp Cell Res*. 2017;350:318-26.
12. Zhao X, Jin Y, Li L, Xu L, Tang Z, Qi Y, et al. MicroRNA-128-3p aggravates doxorubicin-induced liver injury by promoting oxidative stress via targeting Sirtuin-1. *Pharmacol Res*. 2019;146:104276.
13. Yang JH, Lin Y, Guo ZJ, Cheng JK, Huang JY, Deng L, et al. The essential role of MEKK3 in TNF-induced NF- $\kappa$ B activation. *Nat Immunol*. 2001;2:620-4.
14. Padda R, Wamsley-Davis A, Gustin MC, Ross R, Yu C, Sheikh-Hamad D. MEKK3-mediated signaling to p38 kinase and TonE in hypertonically stressed kidney cells. *Am J Physiol Renal Physiol*. 2006;291:F874-81.
15. Feng H, Cao J, Zhang G, Wang Y. Kaempferol Attenuates Cardiac Hypertrophy via Regulation of ASK1/MAPK Signaling Pathway and Oxidative Stress. *Planta Med*. 2017;83:837-45.
16. Qin X, Zhu G, Huang L, Zhang W, Huang Y, Xi X. LL-37 and its analog FF/CAP18 attenuate neutrophil migration in sepsis-induced acute lung injury. *J Cell Biochem*. 2019;120:4863-71.
17. Cheng T, Bai J, Chung CS, Chen Y, Fallon EA, Ayala A. Herpes Virus Entry Mediator (HVEM) Expression Promotes Inflammation/Organ Injury in Response to Experimental Indirect-Acute Lung Injury. *Shock*. 2019;51:487-94.

18. Mo Y, Lou Y, Zhang A, Zhang J, Zhu C, Zheng B, et al. PICK1 Deficiency Induces Autophagy Dysfunction via Lysosomal Impairment and Amplifies Sepsis-Induced Acute Lung Injury. *Mediators Inflamm.* 2018;2018:6757368.
19. Dong A, Yu Y, Wang Y, Li C, Chen H, Bian Y, et al. Protective effects of hydrogen gas against sepsis-induced acute lung injury via regulation of mitochondrial function and dynamics. *Int Immunopharmacol.* 2018;65:366-72.
20. Cadirci E, Ugan RA, Dincer B, Gundogdu B, Cinar I, Akpinar E, et al. Urotensin receptors as a new target for CLP induced septic lung injury in mice. *Naunyn Schmiedebergs Arch Pharmacol.* 2019;392:135-45.
21. Yu X, Li C. Protective effects of propofol on experimental neonatal acute lung injury. *Mol Med Rep.* 2019;19:4507-13.
22. Yao L, Sun T. Glycyrrhizin administration ameliorates *Streptococcus aureus*-induced acute lung injury. *Int Immunopharmacol.* 2019;70:504-11.
23. Fu C, Dai X, Yang Y, Lin M, Cai Y, Cai S. Dexmedetomidine attenuates lipopolysaccharide-induced acute lung injury by inhibiting oxidative stress, mitochondrial dysfunction and apoptosis in rats. *Mol Med Rep.* 2017;15:131-8.
24. Meng PZ, Liu J, Hu PS, Tong F. Protective Effect of Dexmedetomidine on Endotoxin-Induced Acute Lung Injury in Rats. *Med Sci Monit.* 2018;24:4869-75.
25. Gu J, Chen J, Xia P, Tao G, Zhao H, Ma D. Dexmedetomidine attenuates remote lung injury induced by renal ischemia-reperfusion in mice. *Acta Anaesthesiol Scand.* 2011;55:1272-8.
26. Xie C, Li Y, Liang J, Xiao J, Zhao Z, Li T. The effect of dexmedetomidine on autophagy and apoptosis in intestinal ischemia reperfusion-induced lung injury. *Chinese journal of tuberculosis and respiratory diseases.* 2015;38:761-4.
27. Zhang Q, Wu D, Yang Y, Liu T, Liu H. Effects of dexmedetomidine on the protection of hyperoxia-induced lung injury in newborn rats. *Int J Clin Exp Pathol.* 2015;8:6466.
28. Cao F, Li Z, WM Ding, Yan L, Zhao QY. LncRNA PVT1 regulates atrial fibrosis via miR-128-3p-SP1-TGF-beta 1-Smad axis in atrial fibrillation. *Molecular Medicine.* 2019;25:7.
29. Wang XY, Zhang XZ, Li F, Ji QR. MiR-128-3p accelerates cardiovascular calcification and insulin resistance through ISL1-dependent Wnt pathway in type 2 diabetes mellitus rats. *J Cell Physiol.* 2019;234:4997-5010.
30. Xiong LL, Tan Y, Ma HY, Dai P, Qin YX, Yang RA, et al. Administration of SB239063, a potent p38 MAPK inhibitor, alleviates acute lung injury induced by intestinal ischemia reperfusion in rats associated with AQP4 downregulation. *Int Immunopharmacol.* 2016;38:54-60.
31. Ma L, Zhao Y, Wang R, Chen T, Li W, Nan Y, et al. 3,5,4'-Tri-O-acetylresveratrol Attenuates Lipopolysaccharide-Induced Acute Respiratory Distress Syndrome via MAPK/SIRT1 Pathway. *Mediators Inflamm.* 2015;2015:143074.
32. Bode JG, Ehrling C and Haeussinger D. The macrophage response towards LPS and its control through the p38(MAPK)-STAT3 axis. *Cell Signal.* 2012;24:1185-94.

Figures

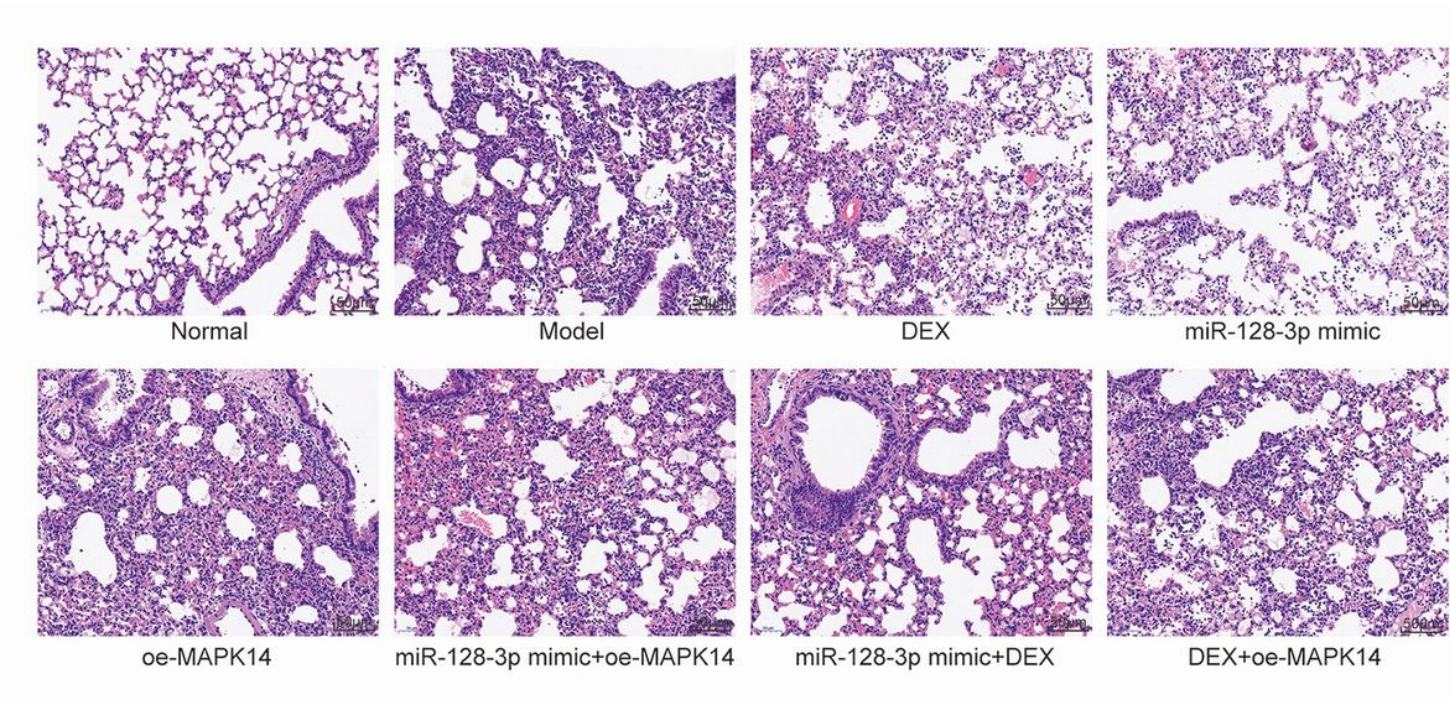


Figure 1

Pathological changes in lung tissue of mice in each group (400×). DEX, dexmedetomidine.

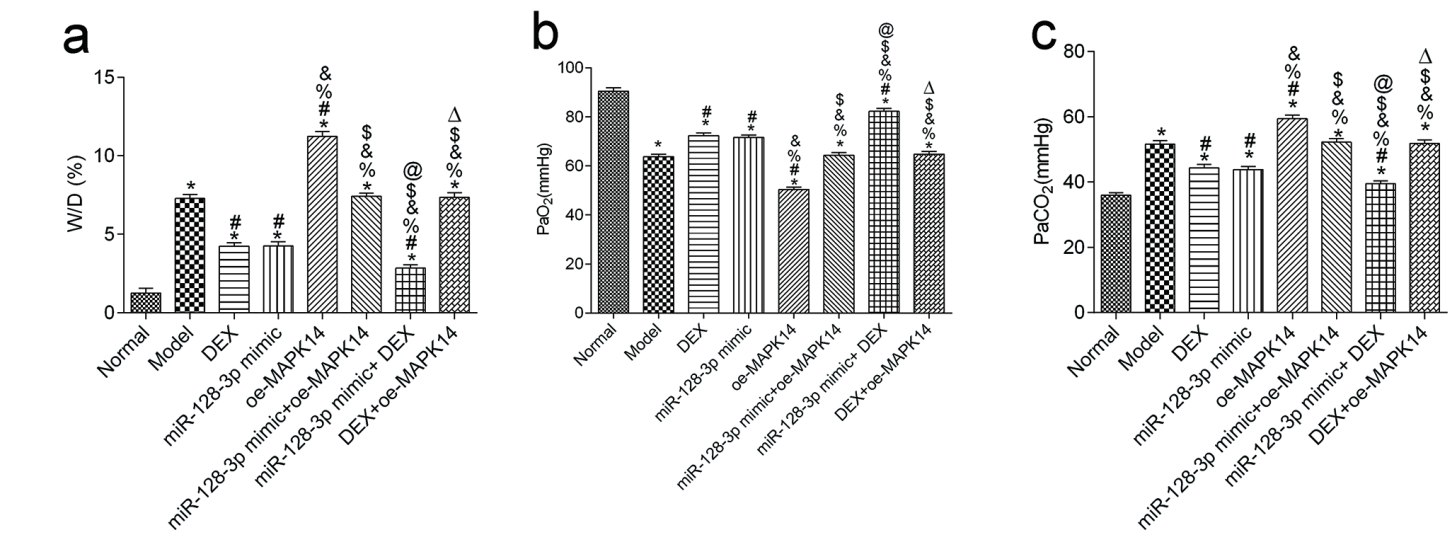


Figure 2

Serum level of inflammatory factors in mice. (a) Serum level of IL-8 in mice; (b) Serum level of IL-17 in mice; (c) Serum level of IL-6 in mice; (d) Serum level of TNF- $\alpha$  in mice. Compared with Normal group, \* $p < 0.05$ ; compared with Model group, # $p < 0.05$ ; compared with DEX group, % $p < 0.05$ ; compared with miR-128-3p mimic group, & $p < 0.05$ ; compared with oe-MAPK14 group, \$ $p < 0.05$ ; compared with miR-128-3p mimic+oe-MAPK14 group, @ $p < 0.05$ ; compared with miR-128-3p mimic+ DEX group,  $\Delta p < 0.05$ . DEX, dexmedetomidine; IL, interleukin; TNF, tumor necrosis factor.

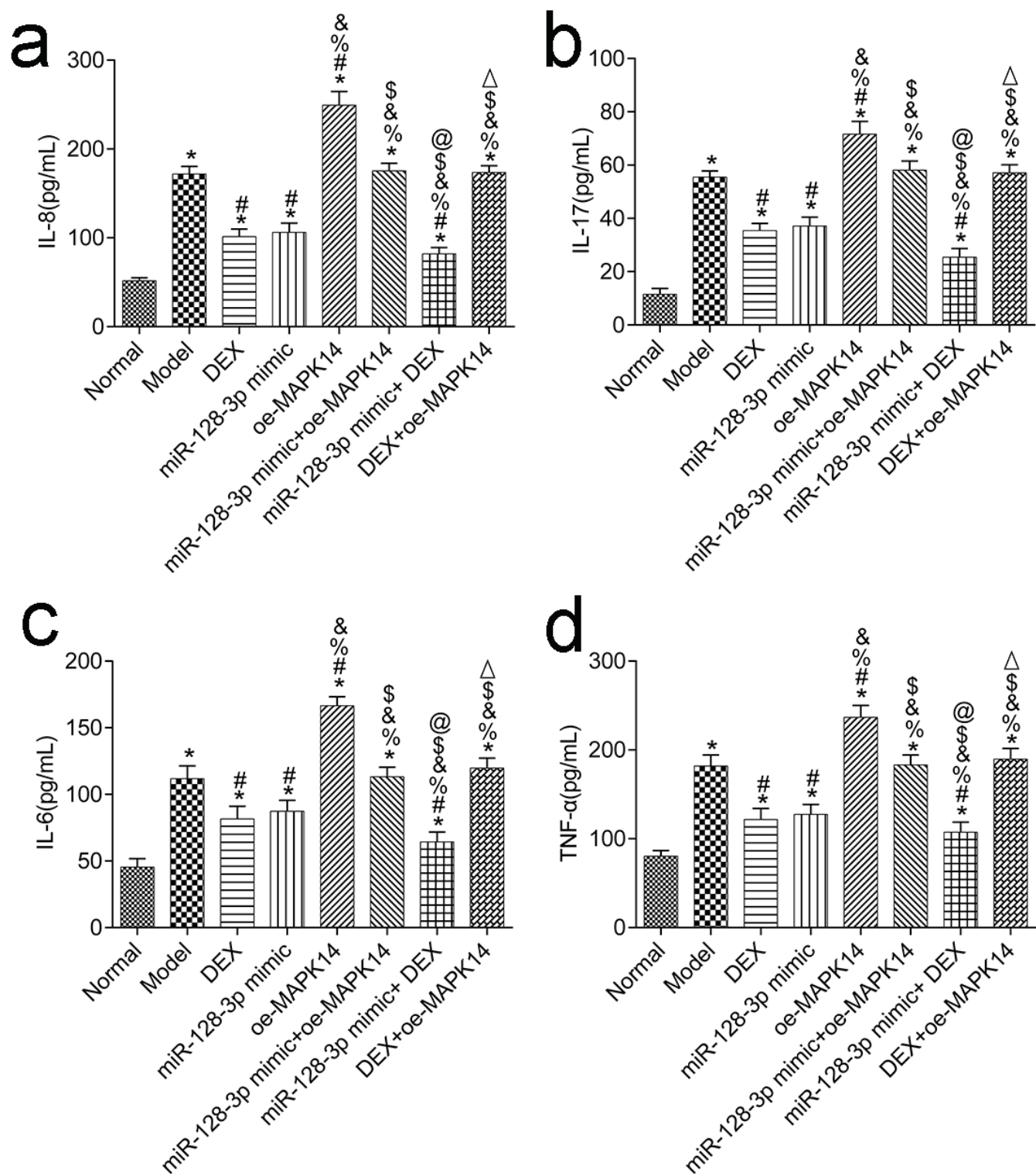
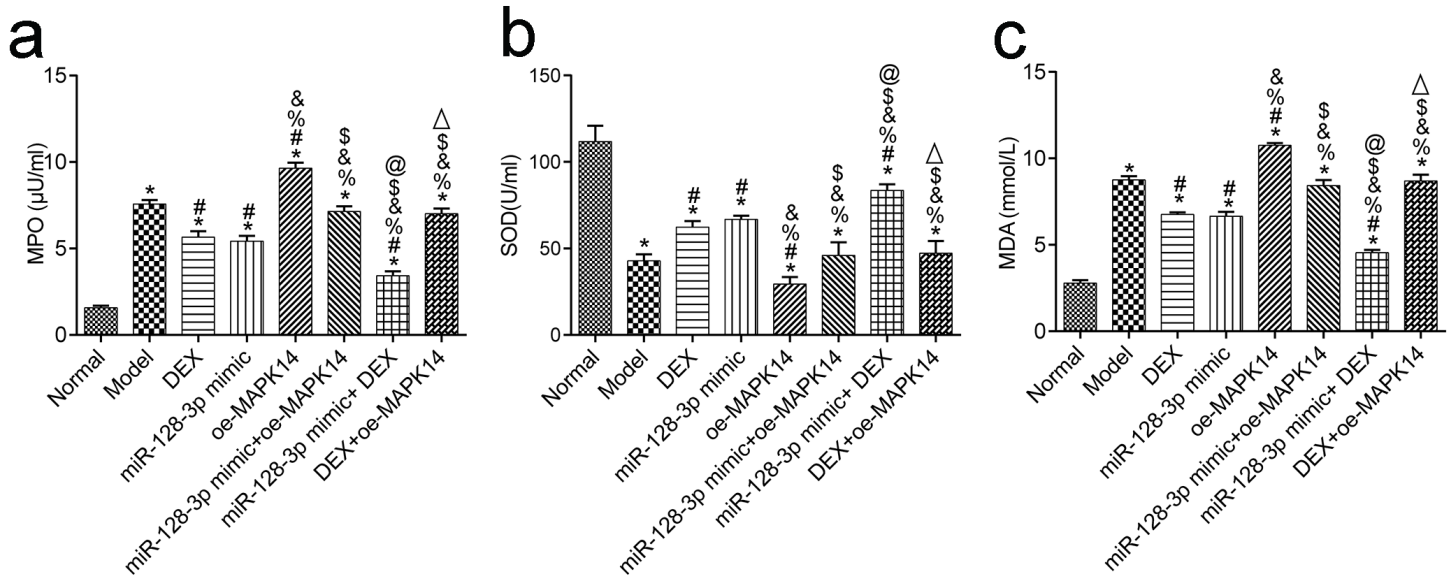


Figure 3

Serum level of inflammatory factors in mice. (a) Serum level of IL-8 in mice; (b) Serum level of IL-17 in mice; (c) Serum level of IL-6 in mice; (d) Serum level of TNF- $\alpha$  in mice. Compared with Normal group, \* $p < 0.05$ ; compared with Model group, # $p < 0.05$ ; compared with DEX group, % $p < 0.05$ ; compared with miR-128-3p mimic group, & $p < 0.05$ ; compared with oe-MAPK14 group, \$ $p < 0.05$ ; compared with miR-128-3p mimic+oe-MAPK14 group, @ $p < 0.05$ ; compared with miR-128-3p mimic+ DEX group,  $\Delta p < 0.05$ . DEX, dexmedetomidine; IL, interleukin; TNF, tumor necrosis factor.



**Figure 4**

MPO, SOD, MDA content in lung tissue of mice in each group. (a) MPO content in mice; (b) SOD content in mice; (c) MDA content in mice. Compared with Normal group, \* $p < 0.05$ ; compared with Model group, # $p < 0.05$ ; compared with DEX group, % $p < 0.05$ ; compared with miR-128-3p mimic group, & $p < 0.05$ ; compared with oe-MAPK14 group, \$ $p < 0.05$ ; compared with miR-128-3p mimic+oe-MAPK14 group, @ $p < 0.05$ ; compared with miR-128-3p mimic+ DEX group,  $\Delta p < 0.05$ . MPO, myeloperoxidase; SOD, superoxide dismutase; MDA, malondialdehyde; DEX, dexmedetomidine.

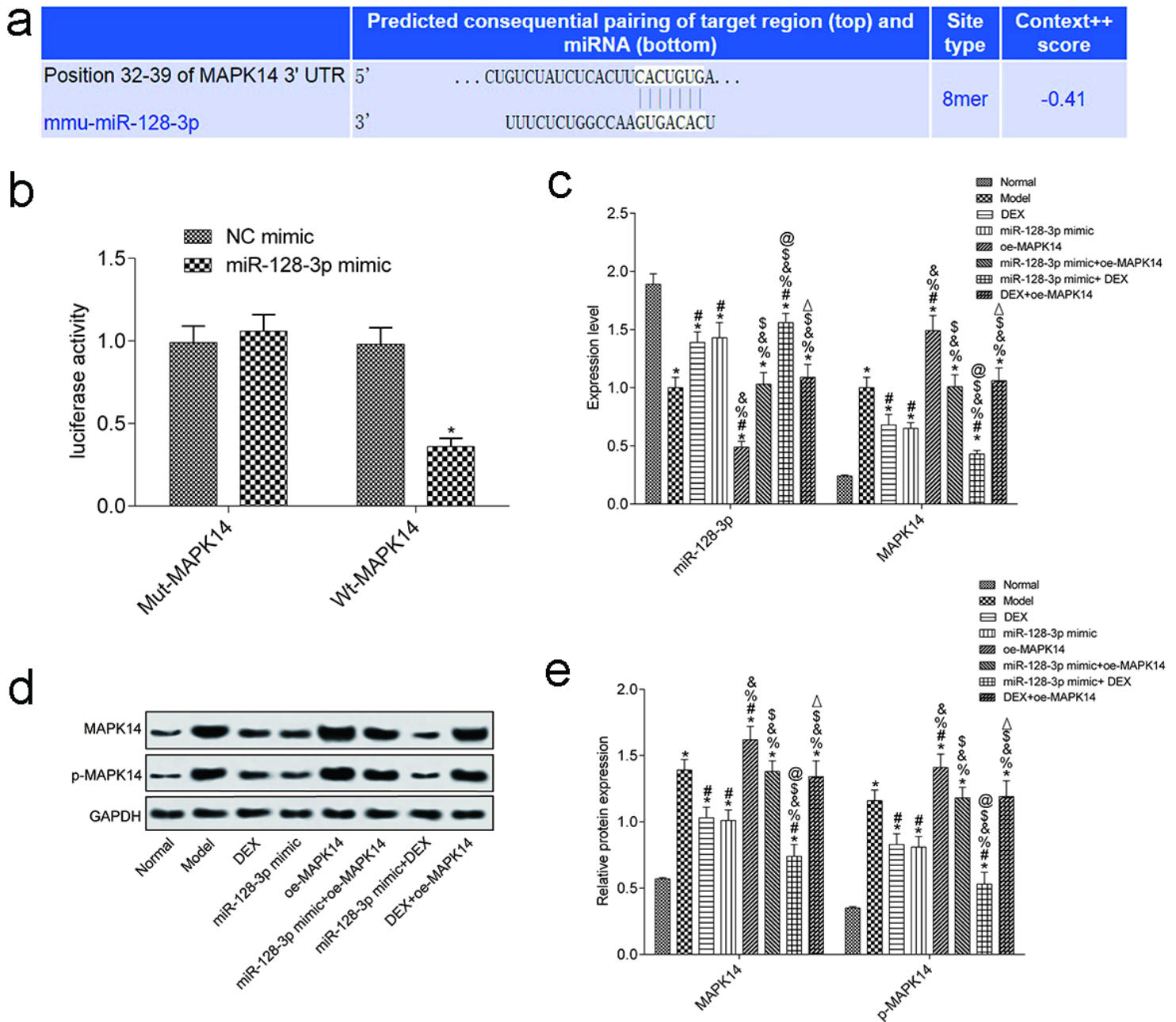


**Figure 5**

miR-128-3p negatively regulates gene expression of MAPK14 and the expression of miR-128-3p and MAPK14. (a) The sequence of the 3'-UTR region in which miR-128-3p binds to MAPK14; (b) Dual luciferase assay to detect luciferase activity. (c) The mRNA levels of miR-128-3p and MAPK14 in lung tissue of each group; (d) The protein bands of MAPK14 and p-MAPK14 in lung tissue of each group; (e) Quantification results of the protein level of MAPK14 and p-MAPK14 in lung tissues of each group. Compared with Normal group, \* $p < 0.05$ ; compared with Model group, # $p < 0.05$ ; compared with DEX group, % $p < 0.05$ ; compared with miR-128-3p mimic group, & $p < 0.05$ ; compared with oe-MAPK14 group,

\$p < 0.05; compared with miR-128-3p mimic+oe-MAPK14 group, @p < 0.05; compared with miR-128-3p mimic+DEX group, Δp < 0.05. DEX, dexmedetomidine. UTR, untranslated region.

## Supplementary Files

This is a list of supplementary files associated with this preprint. Click to download.

- [NC3RsARRIVEGuidelinesChecklistfillable.pdf](#)